

# A cluster with a mixed $M_6X_{12}/M_6X_8$ environment: The $\text{La}_6\text{Cl}_{11}\text{Co}$ structure

Chong Zheng<sup>a,\*</sup>, Hansjürgen Mattausch<sup>b</sup>, Constantin Hoch<sup>b</sup>, Arndt Simon<sup>b</sup>

<sup>a</sup> Department of Chemistry and Biochemistry, Northern Illinois University, DeKalb, IL 60115, USA

<sup>b</sup> Max-Planck-Institut für Festkörperforschung, Heisenbergstrasse 1, D-70569 Stuttgart, Germany

## ARTICLE INFO

### Article history:

Received 28 February 2009

Received in revised form

23 May 2009

Accepted 2 June 2009

Available online 6 June 2009

### Keywords:

Lanthanum

Chloride

Cobalt

Reduced halide

## ABSTRACT

The title compound was synthesized from La,  $\text{LaCl}_3$  and Co under Ar atmosphere at 800 °C. It crystallizes in space group  $P4_2/n$  (no. 86) with lattice constants  $a = 11.308(2)\text{Å}$  and  $c = 14.441(3)\text{Å}$ . The structure features an isolated Co-centered  $\text{La}_6$  octahedron with all corners and edges, and 2 of its 8 triangular faces coordinated by Cl atoms. The  $\text{La}_6\text{Co}$  octahedron is significantly distorted, and the La coordination by Cl atoms deviates from the common close-packing arrangements found in other reduced rare earth metal halides. Structure, bonding and physical properties of the compound have been investigated.

© 2009 Elsevier Inc. All rights reserved.

## 1. Introduction

Reduced rare earth (RE) metal halides have exhibited great chemical hospitality. They can accommodate endohedral atoms ranging from light atoms H and B to heavy ones such as Au and Pb [1–13]. Their structures, however, are based on simple  $RE_6$  trigonal prisms or octahedra. In the latter case, the halide ligands are coordinated to the  $RE_6$  octahedron at the terminal and bridging positions. Thus these structures are derived from the  $M_6X_{12}$  prototype in which all 12 edges of the  $M_6$  octahedron are bridged by the X ligands [1,14–22]. The  $M_6X_8$  coordination type where all 8 faces are capped by the X ligands had not been observed for discrete clusters in the reduced RE metal halide family. Recently, we have reported the first example of a mixed  $M_6X_{12}/M_6X_8$  type,  $\text{La}_6\text{Br}_{10}\text{Fe}$ , in which some coordination environment is derived from the  $M_6X_8$  pattern [23]. In this contribution, we describe the synthesis, structure determination and bonding analysis of a second example with the mixed  $M_6X_{12}/M_6X_8$  environment,  $\text{La}_6\text{Cl}_{11}\text{Co}$ . Its structure features isolated  $\text{La}_6\text{Co}$  octahedra but differs from that of the previously reported compound of similar stoichiometry  $\text{Sc}_6\text{I}_{11}(\text{C}_2)$  [24].

## 2. Experimental section

### 2.1. Synthesis

La metal (sublimed, 99.99%; Alfa-Aesar, small pieces),  $\text{LaCl}_3$  and Co (99.99%; Aldrich) were used as starting materials.  $\text{LaCl}_3$

was prepared by the reaction of  $\text{La}_2\text{O}_3$  with concentrated HCl and  $\text{NH}_4\text{Cl}$ , the product being dried under dynamic vacuum and purified twice by sublimation in a Ta container before use. Due to air and moisture sensitivity of the reactants and product, all handling was carried out under Ar atmosphere either in a glovebox or through the standard Schlenk technique.

The stoichiometric mixture (*ca.* 1.0 g) of the starting materials was arc-sealed in a Ta tube under Ar atmosphere. The Ta tube was then sealed inside a silica glass ampoule under a vacuum of *ca.*  $10^{-2}$  mbar. The reaction was carried out at 800 °C for 16 days. After the reaction, the ampoule was quenched in water and then opened under Ar atmosphere. Many black polyhedral single crystals were observed in the product. The yield, estimated from a Guinier powder X-ray measurement, was approximately 80%. EDX analyses of these single crystals, using a TESCAN scanning electron microscope, confirmed the presence of the component elements in the average atomic ratio of 36(3):58(3):5(3) (La:Cl:Co). The crystals hydrolyze in air within minutes to a white powder.

### 2.2. Structure determination

The reaction product was ground to fine powder under Ar atmosphere and sealed in a glass capillary for phase identification by a modified Guinier technique [25] ( $\text{CuK}\alpha_1$ ;  $\lambda = 1.54056\text{Å}$ ; internal standard Si with  $a = 5.43035\text{Å}$ ; Fujifilm BAS-5000 image plate system). Single crystals were transferred to glass capillaries under Na-dried paraffin oil and sealed under Ar atmosphere. They were first examined by the precession technique before being characterized on a Stoe IPDS diffractometer. Absorption and polarization effect corrections were applied through a

\* Corresponding author.

E-mail address: [czheng@niu.edu](mailto:czheng@niu.edu) (C. Zheng).

face-indexing procedure. The structure was solved with direct methods using the SIR97 program [26]. Full matrix least squares refinement on  $F^2$  was carried out using the SHELXTL package [27].

The product compound crystallizes in the tetragonal space group  $P4_2/n$  (no. 86) with lattice constants  $a = 11.308(2)$  Å and  $c = 14.441(3)$  Å. The structure has been checked for possible existence of higher symmetry by the program ADDSYM in the PLATON package [28]. No additional symmetry element was found. However, the structure could only be refined to  $R_1 = 0.28$ , and the mean  $|E^2 - 1|$  of 0.740 was low for a centrosymmetric space group. A careful examination of the reciprocal lattice and testing for different kinds of twinning laws revealed that by applying a twin matrix of (010; 100; 00-1) the  $R_1$ -factor converged to 0.0443. The two twin components have nearly 1:1 ratio (48% vs. 52%). The crystallographic information including the fractional coordinates and selected bond lengths of the compound using the above twin model is listed in Tables 1–3.

### 2.3. Computational study

The density of states (DOS) and band structure were computed using both the tight-binding extended Hückel method (EH) [29,30] and the self-consistent linear muffin-tin orbital local density approximation method (LDA) as implemented in the Stuttgart-TB-LMTO-ASA program [31]. Sixty-four  $k$ -points in the irreducible wedge of the Brillouin zone were used in the EH computations, and 6  $k$ -points were used during the self-consistent convergence part in the LDA calculations. The EH parameters used in the computation are listed in Table 4. Both EH and LDA methods were used for a comparison of the electronic structures calculated by the two very different programs.

### 2.4. Physical property measurements

For measurement of electrical conductivity, the polycrystalline samples were pressed into pellets of 5 mm in diameter and ca. 2 mm in thickness. The conventional four-contact method [32] was used. Susceptibility measurements were carried out on a Quantum Design PPMS 6000 magnetometer, using sample quantities of ca. 50 mg.

**Table 1**  
Crystal data and structure refinement for  $\text{La}_6\text{Cl}_{11}\text{Co}$ .

Formula weight	1282.34
Temperature	293(2) K
Wavelength	0.56086 Å
Crystal system	Tetragonal
Space group	$P4_2/n$ (no. 86)
Unit cell dimensions	$a = 11.308(2)$ Å $c = 14.441(3)$ Å
Volume	1846.6(5) Å <sup>3</sup>
Z	4
Density (calculated)	4.613 Mg/m <sup>3</sup>
Absorption coefficient	8.396 mm <sup>-1</sup>
$\theta$ Range for data collection	2.64–25.00°
Index ranges	$-17 \leq h \leq 17$ , $-17 \leq k \leq 17$ , $-21 \leq l \leq 21$
Reflections collected	49 315
Completeness to $\theta = 25.00^\circ$	99.9%
Absorption correction	Semi-empirical from equivalents
Data/restraints/parameters	3312/0/86
Goodness-of-fit on $F^2$	1.327
Final $R$ indices ( $I > 2\sigma(I)$ )	$R_1 = 0.0443$ , $wR_2 = 0.1128$
$R$ indices (all data)	$R_1 = 0.0466$ , $wR_2 = 0.1137$
Largest diff. peak and hole	5.944 and $-1.673$ e Å <sup>-3</sup>

**Table 2**  
Atomic coordinates ( $\times 10^4$ ) and equivalent isotropic displacement parameters ( $\text{Å}^2 \times 10^3$ ) for  $\text{La}_6\text{Cl}_{11}\text{Co}$ .

Atom	Wyckoff position	x	y	z	$U(\text{eq})$
La(1)	8g	2365(1)	4825(1)	91(1)	15(1)
La(2)	8g	132(1)	8142(1)	1489(1)	12(1)
La(3)	8g	83(1)	8542(1)	-1264(1)	11(1)
Co	4c	5000	5000	0	7(1)
Cl(1)	8g	32(2)	6465(2)	-64(2)	15(1)
Cl(2)	8g	2362(3)	6112(3)	-1545(2)	23(1)
Cl(3)	8g	2993(2)	5029(3)	2029(2)	21(1)
Cl(4)	4e	2500	7500	835(3)	23(1)
Cl(5)	4f	2500	2500	1064(3)	18(1)
Cl(6)	4f	-2500	7500	1242(3)	28(1)
Cl(7)	8g	-685(3)	9830(3)	2834(2)	24(1)

$U(\text{eq})$  is defined as one third of the trace of the orthogonalized  $U_{ij}$  tensor.

**Table 3**  
Selected bond lengths (Å) up to 3.7 Å and types of Cl atoms for  $\text{La}_6\text{Cl}_{11}\text{Co}$ .

Bonds	Distances	Type <sup>a</sup>
Cl(1)–La(2), –La(3); –La(1), –La(1)	2.919(3), 2.939(3); 3.078(3), 3.232(3)	$e, i-a; a-i$
Cl(2)–La(1), –La(3); –La(2)	2.775(3), 2.944(3); 3.101(3)	$e, i-a; a-i$
Cl(3)–La(1), –La(2), –La(3); –La(3)	2.897(3), 3.064(3), 3.104(3); 3.015(3)	$f, i-a; a-i$
Cl(4)–La(1), –La(2)	3.214(2), 2.931(2)	$e, i-i$
Cl(5)–La(1), –La(3)	2.986(2), 3.1629(8)	$e, i-i$
Cl(6)–La(1), –La(2)	3.262(3), 3.0836(9)	$e, i-i$
Cl(7)–La(2), –La(3); –La(2)	2.876(3), 2.998(3); 2.965(3)	$e, i-a; a-i$
La(1)–Co	2.9895(7)	
La(2)–Co	3.0100(7)	
La(3)–Co	2.4616(6)	
La(1)–La(2)	4.169(1)	
La(1)–La(2)	4.315(1)	
La(1)–La(3)	3.798(1)	
La(1)–La(3)	3.9456(9)	
La(2)–La(3)	3.772(1)	
La(2)–La(3)	4.002(1)	

All bonds have multiplicity of 2.

<sup>a</sup> The notation follows Schäfer and Schneringer [19].  $e$  and  $f$  denote edge bridging and face capping atoms of bridging atom type  $i$ , and  $a$  stands for coordination of corners of adjacent clusters. For example, Cl(4) bridges the La(1)–La(2) edge in one cluster, and the La(1)–La(2) edge in an adjacent one. Thus it is type  $e$ , and in both clusters it acts as a bridging ligand, thus  $i-i$ . Cl(3) caps the La(1)–La(2)–La(3) face, thus it is type  $f$ . It is a terminal ligand to La(3) in an adjacent cluster, thus the notation  $i-a$ . Consider La(3) in the current cluster, it is type  $a-i$ . Therefore a semicolon is used to separate these two types. See Fig. 1.

**Table 4**  
Extended Hückel parameters.

Orbital	$H_{ii}$ (eV)	$\zeta_1^a$	$\zeta_2$	$c_1^a$	$c_2$
La					
6s	-7.67	2.14			
6p	-5.01	2.08			
5d	-8.21	3.78	1.381	0.7765	0.4586
Cl					
3s	-30.0	2.033			
3p	-15.0	2.033			
Co					
4s	-9.21	2.00			
4p	-5.29	2.00			
3d	-13.18	5.55	2.100	0.5680	0.6060

<sup>a</sup> Exponents and coefficients in a double  $\zeta$  expansion of the  $d$  orbital.

### 3. Results and discussion

#### 3.1. Crystal structure

Co-centered  $\text{La}_6$  octahedra are the main structural feature of  $\text{La}_6\text{Cl}_{11}\text{Co}$  (Fig. 1). The  $\text{La}_6\text{Co}$  octahedron is significantly compressed along the  $\text{La}3\text{--Co--La}3$  axis. The apical  $\text{La}3\text{--Co}$  bond length is 2.4616(6) Å, whereas the basal  $\text{La}1\text{--Co}$  and  $\text{La}2\text{--Co}$  bond lengths are 2.9895(7) and 3.0100(7) Å, respectively. This is to be compared with the  $\text{Pr--Co}$  distance of 2.77 of an undistorted octahedron in  $(\text{Ca}_{0.65}\text{Pr}_{0.35})\text{Pr}_6\text{I}_{12}\text{Co}$  [9]. This distortion is similar to that of  $\text{La}_6\text{Br}_{10}\text{Fe}$  where the apical  $\text{La--Fe}$  bond lengths range from 2.414 to 2.547 Å and the basal ones from 2.894 to 3.007 Å. The  $\text{La--La}$  distances vary from 3.77 to 4.31 Å, compared to 3.63–4.26 Å in

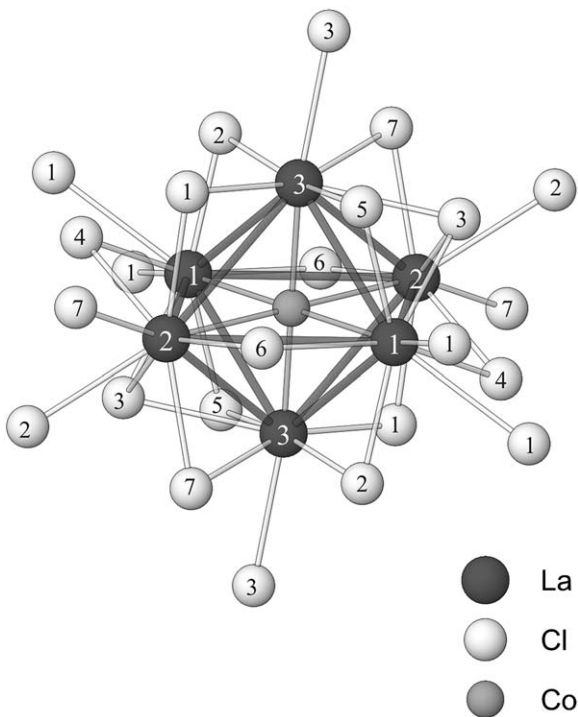


**Fig. 1.**  $\text{La}_6\text{Co}$  octahedron coordinated by Cl atoms in the  $\text{La}_6\text{Cl}_{11}\text{Co}$  structure. Atoms are numbered as in Tables 2 and 3.

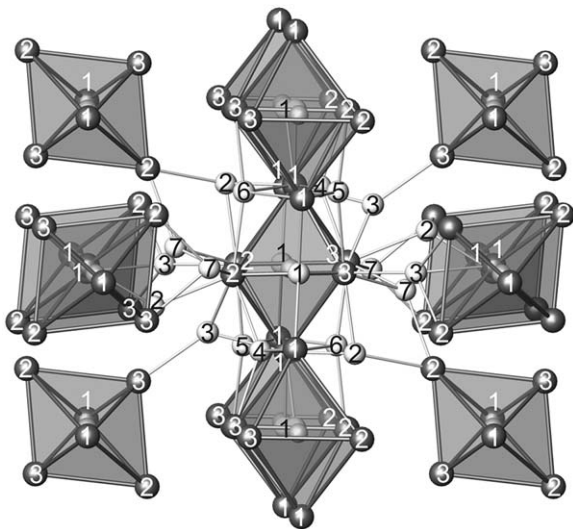


**Fig. 2.** Arrangement of clusters in the structure of  $\text{La}_6\text{Cl}_{11}\text{Co}$  seen in approximate [010] direction.

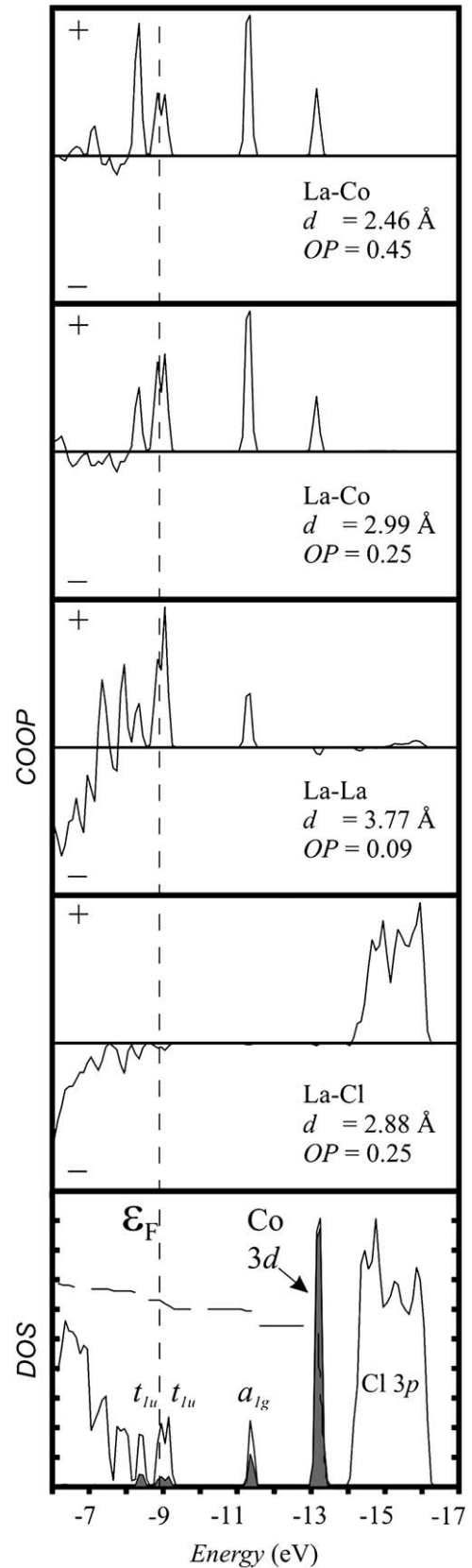


**Fig. 3.** EH DOS and COOP curves of representative bonds in  $\text{La}_6\text{Cl}_{11}\text{Co}$ . In the DOS plot, the solid curves represent the total DOS, the shaded areas and dashed curves correspond to Co contribution and its integrated value, respectively. The vertical dashed line indicates the Fermi level. In the COOP plot, the +region is the bonding and the -region the antibonding area. The bond type, distance and integrated overlap population up to the Fermi level are indicated in each panel.

$\text{La}_6\text{Br}_{10}\text{Fe}$  [23]. The La–Cl distances of 2.77–3.26 Å are within the normal range as in many other reduced rare earth chlorides. They are also comparable to the sum of the ionic radii of  $\text{La}^{3+}$  (1.17 Å for six-coordination and 1.30 Å for eight-coordination) and  $\text{Cl}^-$  (1.67 Å). Four corners of the octahedron ( $\text{La}1 \ 2 \times$  and  $\text{La}2 \ 2 \times$ ) are capped by two and two corners ( $\text{La}3 \ 2 \times$ ) by one Cl atom. All 12 edges are bridged by Cl atoms. In addition, two faces ( $\text{La}1\text{–}\text{La}2\text{–}\text{La}3 \ 2 \times$ ) are capped by Cl atoms, whereas in  $\text{La}_6\text{Br}_{10}\text{Fe}$  three faces are capped.

The capping of the two triangular faces of the  $\text{La}_6\text{Co}$  octahedron is a feature of a mixed  $M_6X_{12}/M_6X_8$  type. The four Cl atoms ( $\text{Cl}2 \ 2 \times$  and  $\text{Cl}7 \ 2 \times$ ) above the basal octahedron apices also bridge the edges of adjacent  $\text{La}_6$  octahedra, and four other basal corner Cl atoms ( $\text{Cl}1 \ 4 \times$ ) are shared among three octahedra. They bridge an edge of a second octahedron and are coordinated to a corner of a third one. The two Cl atoms ( $\text{Cl}3 \ 2 \times$ ) connected to the apical atoms cap the triangular faces of adjacent octahedra. All other bridging Cl atoms ( $\text{Cl}4 \ 2 \times$ ,  $\text{Cl}5 \ 2 \times$  and  $\text{Cl}6 \ 2 \times$ ) also coordinate to the same edges of adjacent  $\text{La}_6\text{Co}$  octahedra (Fig. 2). In contrast to  $\text{La}_6\text{Br}_{10}\text{Fe}$  where eight Br atoms above the corners are shared among three  $\text{La}_6\text{Fe}$  octahedra, in  $\text{La}_6\text{Cl}_{11}\text{Co}$  only six Cl ligands are shared between three  $\text{La}_6\text{Co}$  octahedra.

Neglecting the Cl atoms above the corners, the discrete cluster has the composition  $\text{La}_6\text{Cl}_{12}^e\text{Cl}_2^f\text{Co}$  where  $e$  and  $f$  denote positions above the edges and faces of the octahedron, respectively. As the six  $e$ -type atoms ( $\text{Cl}4 \ 2 \times$ ,  $\text{Cl}5 \ 2 \times$  and  $\text{Cl}6 \ 2 \times$ ) are shared between adjacent clusters in the same functionality, the formula  $\text{La}_6\text{Cl}_6^e\text{Cl}_{6/2}^f\text{Co} = \text{La}_6\text{Cl}_{11}\text{Co}$  follows. In the notation of Schäfer and Schnärer [19] the inter-cluster connection can be described as  $\text{La}_6(\text{Cl}_{4/2}^{a-i-i-a}f)(\text{Cl}_{6/2}^{i-i}\text{Cl}_{8/2}^{i-a-a-i}\text{Cl}_{6/3}^{i-a-a-l,a-i})e\text{Co}$  which also reduces to  $\text{La}_6\text{Cl}_{11}\text{Co}$ .

The closest La–La contact with adjacent octahedra occurs at a distance of 4.942 Å between La1 and La2. Thus there is no La–La bonding between different octahedra. The stacking of these octahedra is different from the known phase of the same stoichiometry  $\text{Sc}_6\text{I}_{11}(\text{C}_2)$  which is derived from the cubic close-packing sequence and crystallizes in the space group  $P\bar{1}$  [24]. It should also be noted there are close Cl–Cl anion contacts between clusters. For example, the Cl(3)–Cl(4) distance is 3.33 Å and Cl(3)–Cl(5) 3.23 Å. However, these distances are common in transition metal or rare earth halides. In  $\text{WCl}_6$ , the shortest Cl–Cl contact is 3.16 Å [33], in  $\text{TbCl}_3$  it is 3.07 Å [34]. In the reduced rare earth halide  $\text{Gd}_3\text{Cl}_6\text{N}$ , it is 3.26 Å [35].

### 3.2. Electronic structure

$\text{La}_6\text{Cl}_{11}\text{Co}$  is isoelectronic to  $\text{La}_6\text{Br}_{10}\text{Fe}$  which has 16 cluster electrons [23]. In the case of an undistorted  $\text{La}_6\text{Cl}_{11}\text{Co}$  octahedral cluster with the Cl atoms above the octahedron edges, 10 of these electrons reside in the Co 3d core, and six in the  $a_{1g}$  and  $t_{1u}$  orbitals that are of La–La bonding character [1,8,9,23,36]. As in the  $\text{La}_6\text{Br}_{10}\text{Fe}$  case, these 16 cluster electrons do not exceed the 18 electron limit imposed by these orbitals. However, since four electrons occupy the degenerate  $t_{1u}$  orbitals in the undistorted cluster, it should be subject to a Jahn–Teller distortion. A compression along the local  $z$ -axis destabilizes one of the three  $t_{1u}$  orbitals that have large Co  $d_{z^2}$  character and stabilizes the remaining two. As we have shown for  $\text{La}_6\text{Br}_{10}\text{Fe}$ , the capping of the two faces will not change significantly the orbital ordering sequence.

Fig. 3 shows the EH DOS and COOP curves for representative contacts in the  $\text{La}_6\text{Cl}_{11}\text{Co}$  structure. As can be seen in the DOS plot, below the Fermi level, all states contribute to La–Cl, La–La and La–Co bonding. The Cl 3p band shows up as a wide peak centered at –15 eV. The Cl 3s band lies low in energy (–30 eV) and is not plotted. The Co 3d band is localized at –13.2 eV. The next higher level in energy is the  $a_{1g}$  derived state which is of La–Co bonding character from the in-phase combination of the La local  $d_{z^2}$  orbital (local  $z$ -axis points to Co) and Co 4s. Just below the Fermi level is a  $t_{1u}$  derived state. It is lower in energy than that of the other two  $t_{1u}$  derived orbitals as a consequence of the compression along the  $z$ -axis of the  $\text{La}_6\text{Co}$  octahedron. Because of the removal of the degeneracy of the  $t_{1u}$  level, a small band gap of ca. 0.2 eV results.

Fig. 4 illustrates the calculated band structure of the  $\text{La}_6\text{Cl}_{11}\text{Co}$  structure using the LDA method where the Fermi level is set to be the zero point of energy. Around –2.3 eV there are four  $a_{1g}$  bands as there are four clusters per unit cell. The relative energy order is slightly different from that of the extended Hückel method. The  $a_{1g}$  bands are below the Co 3d bands. Around the Fermi level, the  $t_{1u}$  bands split into two groups, eight bands are below and four above due to the compression of the  $\text{La}_6\text{Co}$  octahedron. The band gap calculated with the LDA method is approximately 0.8 eV, larger than that estimated by the extended Hückel method. However, both methods give the same qualitative electronic structure of the compound.

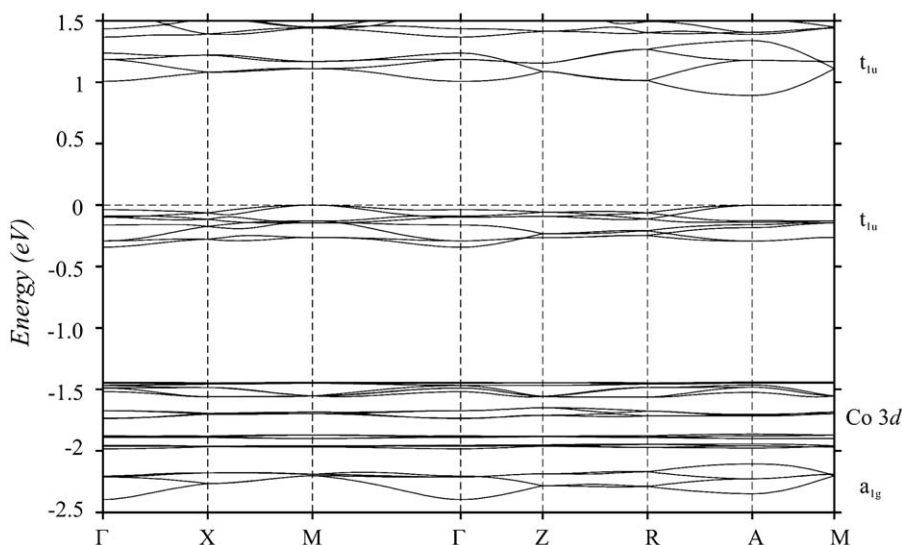


Fig. 4. Band structure of  $\text{La}_6\text{Cl}_{11}\text{Co}$  calculated by the LDA method.

### 3.3. Physical properties

The resistivity measured in the temperature range from 20 to 300 K revealed an insulating behavior with resistivity in the order of  $M\Omega\text{ cm}$ . Both the results of band structure calculation and measurement are in agreement with expectation as the discreteness of the cluster due to interconnection via non-metal atom bridges in all surrounding corners generally results in insulators or semiconductors [21]. The magnetic susceptibility measurement of  $\text{La}_6\text{Cl}_{11}\text{Co}$  revealed essentially non-magnetic behavior, consistent with the closed-shell electron configuration as discussed above. The correction of the measured susceptibility for diamagnetic core contributions leads to temperature independent (van Vleck-type) paramagnetism in the order of  $700 \times 10^{-6} \text{ cm}^3 \text{ mol}^{-1}$  which is a value frequently found for compounds containing discrete  $M_6$  units.

### 4. Conclusions

A second example of a reduced rare-earth metal halide with the mixed  $M_6X_{12}/M_6X_8$  environment,  $\text{La}_6\text{Cl}_{11}\text{Co}$ , has been reported in this manuscript. The synthesis, structure and bonding of the compound are also described. It is possible that more phases of this type exist and deserve to be explored.

### Acknowledgments

We thank V. Duppel for assisting the EDX measurement, E. Brücher for the magnetic susceptibility measurements, G. Siegle for the conductivity measurements, and C. Kamella for help with the drawings.

### References

- [1] A. Simon, H. Mattausch, G.J. Miller, W. Bauhofer, R.K. Kremer, Handbook on the Physics and Chemistry of Rare Earths, vol. 15, Elsevier Science Publishers, Amsterdam, London, New York, Tokyo, 1991, pp. 191–285.
- [2] H. Mattausch, A. Simon, *Angew. Chem. Int. Ed.* 37 (1998) 499–502.
- [3] H. Mattausch, O. Oeckler, A. Simon, *Inorg. Chim. Acta* 289 (1999) 174–190.
- [4] E. Warkentin, A. Simon, *Rev. Chim. Miner.* 20 (1983) 488–495.
- [5] D. Nagaki, A. Simon, H. Borrmann, *J. Less-Common Met.* 156 (1989) 193–205.
- [6] P.K. Dorhout, M.W. Payne, J.D. Corbett, *Inorg. Chem.* 30 (1991) 4960–4962.
- [7] R. Llusar, J.D. Corbett, *Inorg. Chem.* 33 (1994) 849–853.
- [8] T. Hughbanks, G. Rosenthal, J.D. Corbett, *J. Am. Chem. Soc.* 108 (1986) 8289–8290.
- [9] T. Hughbanks, J.D. Corbett, *Inorg. Chem.* 27 (1988) 2022–2026.
- [10] T. Hughbanks, J.D. Corbett, *Inorg. Chem.* 28 (1989) 631–635.
- [11] G. Meyer, M.S. Wickleder, Handbook on the Physics and Chemistry of Rare Earths, vol. 28, Elsevier Science Publishers, Amsterdam, London, New York, Tokyo, 2000, pp. 53–129 (Chapter 177).
- [12] J.D. Corbett, *J. Chem. Soc. Dalton Trans.* (1996) 575–587.
- [13] A. Simon, H. Mattausch, M. Ryazanov, R.K. Kremer, *Z. Anorg. Allg. Chem.* 632 (2006) 919–929.
- [14] R. Chevrel, P. Gougeon, M. Potel, M. Sergent, *J. Solid State Chem.* 57 (1985) 25–33.
- [15] F.A. Cotton, T.E. Haas, *Inorg. Chem.* 3 (1964) 10–17.
- [16] T. Hughbanks, R. Hoffmann, *J. Am. Chem. Soc.* 105 (1983) 3528–3537.
- [17] T. Hughbanks, R. Hoffmann, *J. Am. Chem. Soc.* 105 (1983) 1150–1162.
- [18] J. Köhler, G. Svensson, A. Simon, *Angew. Chem. Int. Ed. Engl.* 31 (1992) 1437–1456.
- [19] H. Schäfer, H.G. Schnering, *Angew. Chem.* 76 (1964) 833–849.
- [20] A. Simon, *Angew. Chem. Int. Ed. Engl.* 20 (1981) 1–22.
- [21] A. Simon, *Angew. Chem. Int. Ed. Engl.* 27 (1988) 159–183.
- [22] G.V. Vajenine, A. Simon, *Inorg. Chem.* 38 (1999) 3463–3473.
- [23] C. Zheng, H. Mattausch, C. Hoch, A. Simon, *Inorg. Chem.* 47 (2008) 2356–2361.
- [24] D.S. Dubis, J.D. Corbett, *Inorg. Chem.* 26 (1987) 1933–1940.
- [25] A. Simon, *J. Appl. Crystallogr.* 3 (1970) 11–18.
- [26] A. Altomare, M.C. Burla, M. Camalli, G.L. Cascarano, C. Giacovazzo, A. Guagliardi, A.G.G. Moliterni, G. Polidori, R. Spagna, *J. Appl. Crystallogr.* 32 (1999) 115–119.
- [27] G.M. Sheldrick, SHELXTL Version 6.10, Bruker Analytical Instruments, Madison, Wisconsin, 2000.
- [28] A.L. Spek, *Acta Crystallogr. Sect. A Found. Crystallogr.* 46 (1990) C34.
- [29] R. Hoffmann, *J. Chem. Phys.* 39 (1963) 1397–1412.
- [30] M.H. Whangbo, R. Hoffmann, R.B. Woodward, *Proc. R. Soc. London A366* (1979) 23–46.
- [31] O.K. Andersen, O. Jepsen, *Phys. Rev. Lett.* 53 (1984) 2571–2574.
- [32] L.J. Pauw, *Philips Res. Rep.* 13 (1958) 1–9.
- [33] J.C. Taylor, P.W. Wilson, *Acta Crystallogr. B* 30 (1974) 1216–1220.
- [34] J.D. Forrester, A. Zalkin, D.H. Templeton, J.C. Wallmann, *Inorg. Chem.* 3 (1964) 185–188.
- [35] A. Simon, T. Koehler, *J. Less-Common Met.* 116 (1986) 279–292.
- [36] L.E. Sweet, L.E. Roy, F. Meng, T. Hughbanks, *J. Am. Chem. Soc.* 128 (2006) 10193–10201.